A Telescopic Independent Component Analysis on Functional Magnetic Resonance Imaging Data Set

Shiva Mirzaeian[1,2*], Ashkan Faghiri[1], Vince D. Calhoun[1,2,3,4], Armin Iraji[1,3*]

[1]Tri-Institutional Center for Translational Research in Neuroimaging and Data Science (TReNDS), Atlanta, GA, USA

[2]Department of Mathematics and Statistics, Georgia State University, Atlanta, GA, USA

[3]Department of Computer Science, Georgia State University, Atlanta, GA, USA

[4]Neuroscience Institute, Georgia State University, Atlanta, GA, USA

* Correspondence address to:

Smirzaeian1@gsu.edu (Shiva Mirzaeian)

airaji@gsu.edu (Armin Iraji)

Abstract:

Brain function can be modeled as the dynamic interactions between functional sources at different spatial scales, and each spatial scale can contain its functional sources with unique information, thus using a single scale may provide an incomplete view of brain function. This paper introduces a novel approach, termed "Telescopic independent component analysis (ICA)," designed to construct spatial functional hierarchies and estimate functional sources across multiple spatial scales using fMRI data. The method employs a recursive ICA strategy, leveraging information from a larger network to guide the extraction of information about smaller networks. We apply our model to study the default mode network (DMN) and evaluate the difference between healthy people and individuals with schizophrenia. We show that the telescopic ICA approach can detect the spatial hierarchy of DMN and their associated group differences between cohorts that may not be captured if we focus on a single-scale ICA. In sum, our proposed approach represents a promising new tool for studying functional sources.

Keywords: Multi-spatial-scale intrinsic connectivity networks, independent component analysis (ICA), Resting-state functional magnetic resonance imaging (fMRI), schizophrenia.

1. Introduction:

1.1. Intrinsic connectivity networks:

A Macroscopic brain's function can be conceptualized as coordination and interaction among functional sources, a model incorporating the fundamental principles of segregation and interaction (Genon et al., 2018; Armin Iraji et al., 2022). From this perspective, the brain is comprised of distinct functional sources that dynamically interact with each other. These functional sources can be characterized by temporally synchronized patterns, which can be assessed at the macroscale using resting-state functional magnetic resonance imaging (rs-fMRI) and techniques such as independent component analysis (ICA)(Calhoun & Adalı, 2012; van den Heuvel & Hulshoff Pol, 2010). ICA is a robust blind source separation technique that separates complex rs-fMRI signals into spatial patterns that are temporally coherent and maximally independent of each other (Calhoun & Adalı, 2012; Calhoun et al., 2001; Calhoun & de Lacy, 2017). These spatial patterns and associated time courses formed the estimation of functional sources and are commonly referred to as intrinsic connectivity networks (ICNs) (Allen et al., 2014). Importantly, these ICNs can be captured at different spatial scales (Abou-Elseoud et al., 2010; Armin Iraji et al., 2022; Iraji et al., 2023). Previous research has underscored the significance of the analysis of ICNs at multiple spatial scales (Armin Iraji et al., 2022; Li et al., 2018; Meng et al., 2022; Meng et al., 2023). Previous studies that explore multiple spatial scales can be divided into two major categories. The category relies on a singular set of nodes, such as predefined regions or a single model-order ICA, to reconstruct different scales of functional hierarchy using various modularity or clustering techniques (Doucet et al., 2011); however, these approaches have no information that can be explained by looking at the other spatial scales. The other category of approaches appreciates that ICNs at different spatial scales can contain distinctive functional sources with their unique information. For instance, previous studies utilized ICA with different model orders to capture ICNs at different spatial scales to study whole-brain functional connectivity (Armin Iraji et al., 2022; Meng et al., 2022). Lower model order yields large-scale, spatial distributed ICAs (Beckmann et al., 2005; Calhoun et al., 2008; Iraji et al., 2016) while higher model orders result in more finely-grained, spatially specific ICNs (E. Allen et al., 2011). Importantly, the interaction between large-grained scale and small-grained scale can convey crucial insights into the brain's functioning. for instance, multiscale brain analysis better captures sex-specific schizophrenia changes (Armin Iraji et al., 2022). However, these techniques require post hoc analysis to construct

the spatial hierarchy and assign ICNs to different spatial scales, as the method does not impose direct constraints on the size of ICNs.

Here, we present a new ICA strategy, called telescopic ICA, to construct spatial functional hierarchy and estimate ICNs across multiple spatial scales. The approach is essentially a recursive technique that leverages ICNs from the previous scale to guide the ICA to obtain ICNs for another scale. Notably, our approach is designed to show how a large-scale network decomposes through a small-scale network using zooming in based on the prior level of the functional source.

1.2. Schizophrenia:

Schizophrenia represents a psychotic disorder characterized by different cognitive impairments and a decline in both social and occupational functioning(Association, 2013; Van Den Heuvel & Fornito, 2014). This condition is multifaceted, diagnosed through a syndromic approach, and involves excluding other potential diagnoses. Schizophrenia lacks distinctive symptoms and is primarily diagnosed based on clinical observations of positive symptoms (such as delusions, hallucinations, disorganized speech, and disorganized or catatonic behavior) as well as negative symptoms (including apathy, blunted affect, and anhedonia), along with a noticeable deterioration in social functioning(Association, 2013). Schizophrenia exhibits substantial overlap with both schizoaffective disorder and psychotic bipolar disorder, in both symptoms, genetic factors, and other biomarkers(Clementz et al., 2016). Schizophrenia is theorized to be a developmental disorder marked by disrupted brain function, characterized by either functional dysconnectivity or alterations in functional integration(Friston & Frith, 1995; Kahn et al., 2015). research also has elucidated sex differences in the incidence and clinical manifestation of mental disorders (Dalsgaard et al., 2020; Paus et al., 2008). Females with schizophrenia tend to show more depressive symptoms, whereas males often experience more negative symptoms (Ochoa et al., 2012). Also, recent studies highlight the importance of analyzing the brain in multiscale to capture sex-specific schizophrenia changes (Armin Iraji et al., 2022); and previous studies have shown high-order functional connectivity applied to the diagnosis of psychotic disorders (Herzog et al., 2022; Li et al., 2023). Therefore, studying brain functional sources at different scales can provide crucial information about brain functional integration and its schizophrenia changes, potentially improving our understanding of the actual brain pathology underlying different schizophrenia subcategories. Here we used the telescopic ICA approach to identify the spatial map of the default

mode network (DMN) in two scales and provide important information about brain functional sources and its schizophrenia changes, potentially improving our understanding of the actual brain pathology, thus eventually improving treatments and care for individuals with schizophrenia. Our results show that the telescopic ICA approach can capture significant group differences in DMN area between healthy people (HC) and schizophrenia patients (SZ) which are missed in single-scale ICA.

2. Materials and methods:

2.1. Proposed approach:

In our proposed approach, first, we applied two levels of principle component analysis (PCA) followed by group level ICA (GICA) on a data set (Calhoun et al., 2009; Erhardt et al., 2011). Subject spatial PCA at the first level applied to normalize the data and to allow subjects to contribute similarly to the common subspace. It also has denoising and computational benefits using the equation:

$$Y_i = F_i^{-} Y_i \qquad (Eq1)$$

Here subject-specific BOLD signal Y_i is T_1-by-V reduced data for a subject i, F_i^{-} is the T_1-by-T standardized reducing matrix.T_1 is the number of PCs retained for each subject, T is total number of time points and V is the number of voxels. While the subject-specific PCA privileges subject differences at the subject level, the group-level PCA favors subject commonalities(Erhardt et al., 2011). All subject-level principal components were concatenated together across the time dimension, and group-level spatial PCA was applied to concatenated subject-level principal components($Eq2, Eq3$).

$$Y = \begin{bmatrix} Y_1 \\ \vdots \\ Y_M \end{bmatrix} = \begin{bmatrix} F_1^{-} Y_1 \\ \vdots \\ F_M^{-} Y_M \end{bmatrix} \qquad (Eq2)$$

$$X \equiv G^{-}Y = [G_1^T, \dots, G_M^T] \begin{bmatrix} F_1^{-}Y_1 \\ \vdots \\ F_M^{-}Y_M \end{bmatrix} = \sum_{i=1}^{M} G_i^T F_i^T Y_i = \sum_{i=1}^{M} X_i \qquad (Eq3)$$

Here M is number of subjects, and G^{-} is the T_2 by MT_1 standarized reducing matrix. Group-level principal components that explained the maximum variance were selected as the input for spatial ICA to calculate group independent components. We express the relationship as:

$$X = \hat{A}\hat{S} \qquad (Eq4)$$

where the generative linear latent variables $\hat{A}$ and $\hat{S}$ are the $T_2 \times T_2$mixing matrix related to subject time courses and the $T_2 \times V$ aggregate spatial maps, respectively. In our proposed approach we modified $(Eq4)$ as

$$X \odot W = \hat{A}_j^k \, \hat{S}_j^k \qquad (Eq5)$$

$$W = \hat{S}_{j-1}^k \qquad (Eq6)$$

Where $\hat{S}_{j-1}^k$ represent k^{th}spatial map from $(j-1)^{th}$ scale, and $\odot$ is vector outer product. In the first scale, we select $W = 1$ as there is no previous scale ($j = 0$). In our proposed approach, group spatial ICA (GICA) was applied on the weighted signals (voxel wise multiplication of a network on the BOLD signal), leading to the identification of the networks at the next scale. (Figure 1)

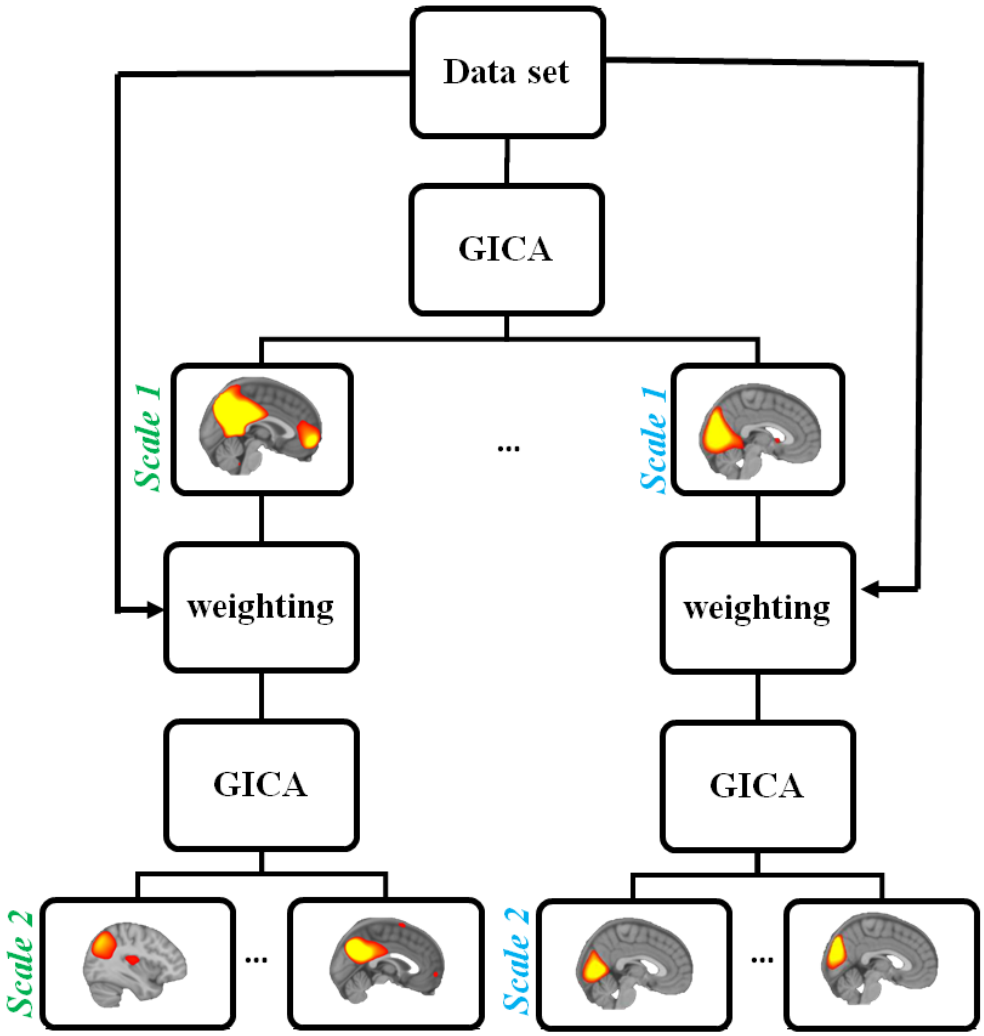

Figure 1: Introducing Telescopic independent component analysis (ICA): a novel approach for identifying ICNs at the multis-scale level. In each scale group-level spatial ICA(GICA) was applied on the weighted signal (voxel wise multiplication of a network on the BOLD signal), leading to the identification of the network at the next scale. In the first scale, as there is no previous scale, GICA applied on the original BOLD signal.

2.2. Demographics and data acquisition:

In this study, we utilized data from the Functional Imaging Biomedical Informatics Research Network (FBIRN) data set for our investigation (Potkin & Ford, 2009). The FBIRN dataset was collected from seven sites. The same rs-fMRI parameters were used across all sites: a standard gradient echo-planar imaging (EPI) sequence, repetition time (TR)/echo time (TE) = 2,000/30 ms, voxel spacing size = 3.4375 × 3.4375 × 4 mm, slice gap = 1 mm, flip angle (FA) = 77°, field of

view (FOV) = 220 × 220 mm, and a total of 162 volume. Six of the seven sites used 3-Tesla Siemens Tim Trio scanners, and one used a 3-Tesla General Electric Discovery MR750 scanner. The dataset was chosen using the following quality control: (a) individuals diagnosed with either typical control or schizophrenia conditions, (b) data demonstrating high-quality registration to the EPI template, (c) minimal head motion characterized by less than 3° rotations and 3-mm translations in every direction, and (d) mean framewise displacement less than 0.2. Consequently, our analysis was performed on rs-fMRI data derived from 310 individuals, comprising 150 HC and 160 SZ, as summarized in Table 1. All participants are also at least 18 years old and gave written informed consent prior to enrollment.

Project	Diagnostic	Number	Sex	Number	Age(years) Mean ± STD Median/Range	
FBIRN	Healthy group	160	Male Female	115 45	37± 10.71 36.47±11.33	39(19-59) 33/ (19-58)
	Schizophrenia group	150	Male Female	114 36	38.74±11.78 39.06±11.40	40/ (18-62) 36/ (21-57)

Table 1: Demographic information of the data used in the Functional Imaging Biomedical Informatics Research Network (FBIRN) study.

2.3. Analysis pipeline:

The re-fMRI data preprocessing was conducted using the Statistical Parametric Mapping toolbox (SPM12, https://www.fil.ion.ucl.ac.uk/spm/). Preprocessing steps include discarding the initial five volumes, rigid motion correction, and slice-time correction. Subsequently, individual subject data were registered to an MNI EPI template, resampled, and smoothed with a 6mm Gaussian Kernal, and variance normalization was applied on voxel time (Armin Iraji et al., 2022).

We used the GIFT toolbox https://trendscenter.org/software/gift/ (Calhoun & Adalı, 2012; Calhoun et al., 2001; Iraji et al., 2021) to apply the telescopic ICA. To begin, the 30 PCs that explained the maximum variance of each subject and the 20 group-level PCs that explained the maximum variance of each estimator-specific data set were used as the input for spatial GICA. We

selected a spatial GICA model order of 20 to obtain large-scale ICNs (Iraji et al., 2016; Iraji et al., 2019). For the GICA algorithm, we used the infomax algorithm (Bell & Sejnowski, 1995; Lee et al., 1999) ran it 100 times, and utilized the ICASSO framework to identify the best estimate, defined as the independent component closest to the stable cluster (Himberg et al., 2004). We employed back-reconstruction using GICA technique (Calhoun et al., 2001) to compute subject-specific independent component and time courses because it provides more accurate time courses and spatial maps.

Afterward, we employed a selection process for identifying the DMN. We identified the DMN using prior knowledge and the following criteria (a) dominant low-frequency fluctuations in their time courses, determined through dynamic rage assessment and the low-frequency to high-frequency power ratio;(b) peak activation located within gray matter regions;(c) minimal spatial overlap with vascular and ventricular structures and (d) low spatial similarity with motion and other recognized artifacts (E. Allen et al., 2011). Next, we performed the weighting step for all subjects' BOLD signals with the DMN spatial map of scale 1. Finally, we applied the GICA on the weighted BOLD signals. Similar to the previous scale, we applied 2 levels of PCA. In subject level 6 PCs, and in group-level 4 PCs that explained the maximum variance of data set were used to input for GICA. Since prior research does not exist, we select the model order of GICA using the elbow criterion to determine the optimal number of PCs. All other parameters in GICA to extract DMN scale 2 are the same as scale1.

2.4. Accessing the replicability of telescopic ICA approach- pipeline evaluation:

We evaluated the replicability (Adali et al., 2022; National Academies of Sciences et al., 2019) of our approach using the initial random division of the dataset into two distinct subsets, each of which underwent independent processing through our pipeline. This division and processing were repeated 100 times, with each iteration yielding one DMN scale 1 and its corresponding four zoomed-in DMN, extracted from scale 2. To quantify the replicability of our approach, we calculated the average of spatial similarity between each pair of ICN from two independent half splits using the Pearson correlation (Figure 2).

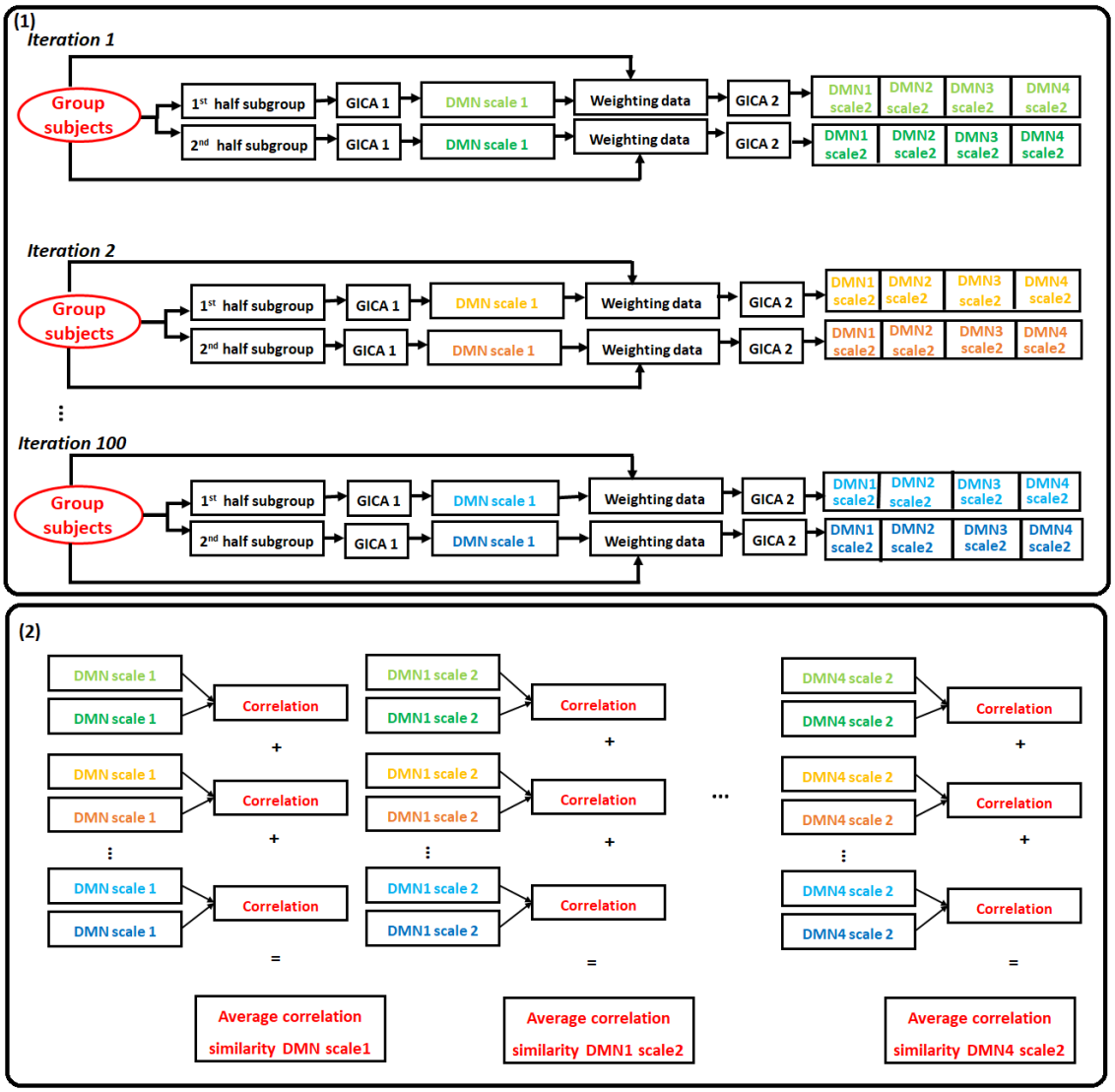

Figure 2: Pipeline to assess the replicability of the telescopic ICA approach. First, the dataset was divided into two separate subsets randomly. Each of these subsets was subjected to independent processing through the Telescopic ICA approach. This division and processing procedure were repeated 100 times, leading to the extraction of the DMN from scale 1 and its corresponding four zoomed-in DMN obtained from scale 2. Finally, the average spatial similarity was calculated by using the Pearson correlation for every pair of networks within the two subsets.

We also assessed the correlation similarity between individual-level and group-level DMN, and correlation similarity between individual- level DMN within scale 1 and scale 2. To accomplish this, we obtained the DMN for each participant and subsequently computed the

Pearson correlation between the group-level DMN and corresponding individual DMN to get the similarity in group and individual-level. We also calculated the Pearson correlation between individual subjects and obtained the similarity in individual-level. This comparative analysis was performed for both scale 1 and scale 2 DMN, providing a comprehensive examination of the similarity between individual-level and individual-level and group-level DMN at both scales.

2.5. Group comparison analysis:

To assess ICN differences between HC and SZ, we first identified the voxels with a strong contribution to a given ICA (Z>1.96). We next conducted voxel-wise two-sample t-tests and applied an adaptive thresholding technique based on the Gamma-Gaussian mixture model (Gorgolewski et al., 2012)to identify voxels with significant diagnostic effects.

2.6. High order GICA:

To investigate the comparison of DMN components derived through telescopic ICA method using a single scale ICA, we conducted ICA with a high model order on FBIRN data set. The GICA analysis steps are as follows. First, 120 PCs that explained the maximum variance of each subject were retained for further analysis. Next, 80 group-level PCs that explained the maximum variance of each estimator-specific data set were used as the input for GICA. We applied model order 80 as GICA high order; The model order choice was motivated by the telescopic ICA procedure, where we initially employed GICA with a model order of 20 to get networks in scale 1, then an additional GICA with a model order of 4 used to get smaller networks in scale 2. For the high model order GICA algorithm, similar to telescopic approach, we used the infomax algorithm, the ICASSO framework, and GICA back-reconstruction techniques compute subject-specific independent component and time courses. Afterward, we employed a selection process for identifying the DMN like telescopic ICA approach. To quantify the similarity between DMN from telescopic ICA and high order GICA, we calculated spatial similarity using Pearson correlation. We also applied group comparison analysis for DMN derived from high order GICA. Similar to telescopic ICA approach, we identified the group effect in voxels that significantly contribute to DMN in HC and SZ groups and using an adaptive thresholding technique to identified regions with significant diagnostic effects.

3. Results:

3.1. The default mode network hierarchy:

According to the criteria specified in the materials and methods section, we identified DMN extracted from scale 1, along with its four 'zoomed in' DMN derived from scale 2. The decomposition of the DMN across these two spatial scales is visually depicted in (Figure 3). In DMN scale 1, the number of voxels that significantly contribute (Z > 1.96) are 2948. In DMN scale2, the significant voxels are 1077, 2723, 965, and 1426 respectively. This shows that telescopic approach captures bigger networks in scale 1 and smaller network in scale2. In addition, the spatial correlation similarities between DMN scale1 with DMN scale2 are 0.43, 0.61, 0.42, and 0.61 respectively. These results show that the telescopic approach can capture distinctive networks in each scale.

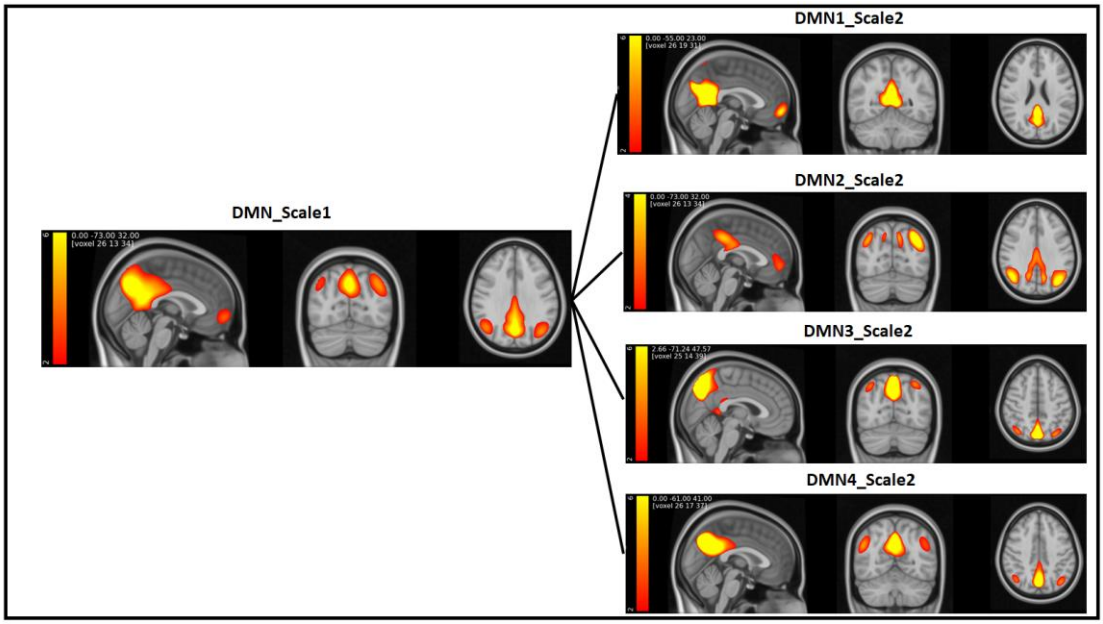

Figure 3: Visualization of DMN spatial maps extracted from telescopic ICA approach. It shows the decomposition of the DMN in scale 1 in scale 2. The spatial correlation similarities between DMN scale1 with DMN scale2 are 0.43, 0.61, 0.42, and 0.61 respectively.

3.2. Replicability of analysis:

(Figure 4) displays the Pearson correlation coefficient between the DMN in scale 1 and scale 2 across the first and second halves of the data set over 100 iterations. The replicability index

(average spatial similarity across 100 iterations) for all ICNs is well above 0.8. The DMN scale 1 exhibited a reliability of 0.97 with a standard deviation of 0.01. The DMN generated in scale 2 also yielded replicability with values of 0.80, 0.83, 0.91, and 0.81 along with corresponding standard deviations of 0.20, 0.18, 0.06, and 0.24, respectively. Lower average similarity in scale 2 compared with scale 1 indicated some variability in more detailed functional sources. This outcome aligns with the observed pattern in a high model order ICA approach (Abou-Elseoud et al., 2010).

We also present the similarity between individual-level DMN spatial map as well as individual-level and group-level DMN spatial map generated from the telescopic ICA approach using Pearson correlation coefficient. The computed average similarities between group level and individual level in scale 1 was 0.54, and in scale 2 are 0.60, 0.72, 0.70, and 0.69, respectively. Also, the average Pearson correlation coefficient in individual-levels from DMN scale 1 and DMN scale 2 are 0.30, 0.37, 0.52, 0.49, 0.48. Standard deviations of correlation similarity in subject level are 0.09, 0.17, 0.18, 0.17, and 0.18 respectively. The visual representation in (Figure 4) illustrates the boxplot of these similarities, revealing a higher similarity in DMN scale 2 as compared to DMN scale 1.

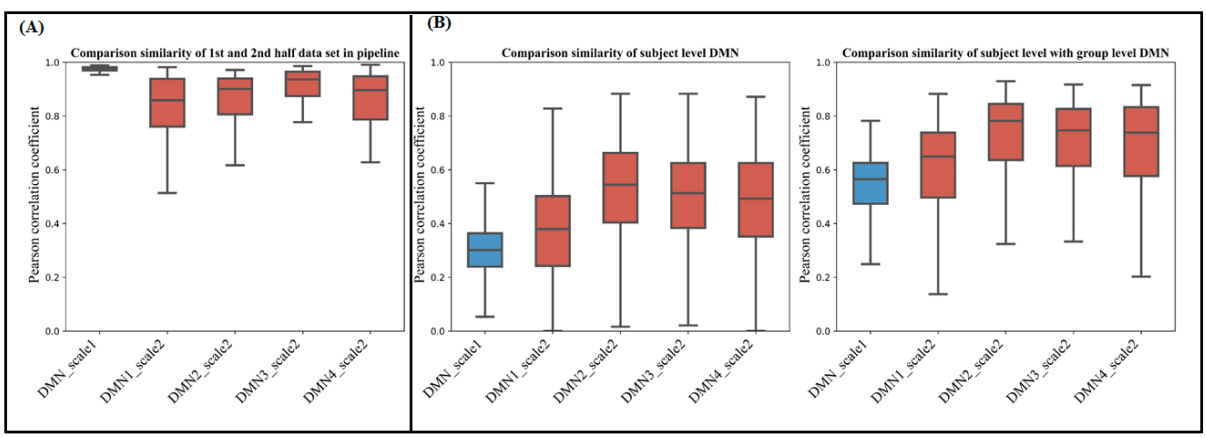

Figure 4: (A) The box plot displays the Pearson correlation coefficient between the first half and second half of dataset, providing insights into the pipeline's replicability. The average similarities of all components are higher than 0.8. (B) The boxplot represents the Pearson correlation

coefficient between subject-level DMN, and subject-level DMN and group-level DMN. The average similarity in scale 2 is higher than scale1 in both case comparison.

3.3. Clinical applications:

(Figure 5)illustrates the t-map of voxels with significant diagnostic effects ($p < 0.01$) after adoptive thresholding using Gamma-Gaussian mixture model. Notably, the maps revealed significant group differences in the DMN scale2, which were not evident in scale1. In DMN scale 1, the areas exhibiting significant differences include the middle cingulate and paracingulate gyri, posterior cingulate gyrus, cuneus, lingual gyrus, middle occipital gyrus, angular gyrus, and precuneus. Conversely, in DMN scale 2, significant differences beside the area in scale1 are manifested in the superior frontal gyrus, medial orbital, calcarine fissure and surrounding cortex, superior occipital gyrus, and inferior parietal gyrus.

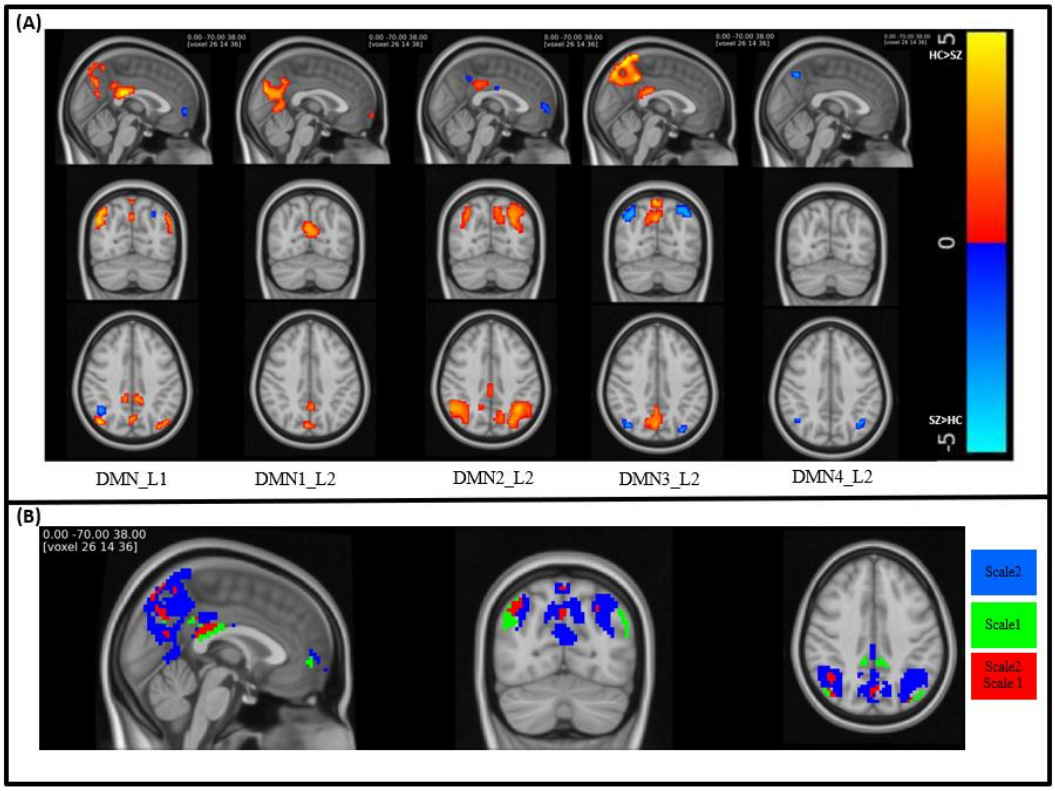

Figure 5: (A)visualization of T-map of brain regions show significant group differences ($p < 0.01$) between HC and SZ under telescopic ICA approach. (B)Visualization of significant voxels in both scale 1 and scale 2(red), only scale 1(green), and only scale 2(blue).

3.4. GICA high order:

We identified four distinct DMN extracted through ICA at order 80. (Figure 6) displays the spatial maps of these DMNs, denoted as DMN1, DMN2, DMN3, and DMN4. Subsequently, we assessed the correlation similarity between DMN1 and DMN generated from a telescopic approach, revealing values of (0.30, 0.13, 0.35, 0.10, 0.18). Similar correlation assessments were conducted for DMN2 (0.71, 0.57, 0.15, 0.19, 0.73), DMN3 (0.40, 0.01, 0.007, 0.50, 0.44), and DMN4 (0.25, 0.10, 0.19, 0.04, 0.08). Additionally, (Figure 6) presents the outcomes of significant group differences between a HC and SZ, derived from all DMN at a high model order. The identified areas exhibiting significant group differences encompass the inferior parietal gyrus, angular gyrus, precuneus, and cuneus regions. The number of significant voxels in DMN from ICA order 80 are revealed as 49, 46, 32, and 14, respectively.

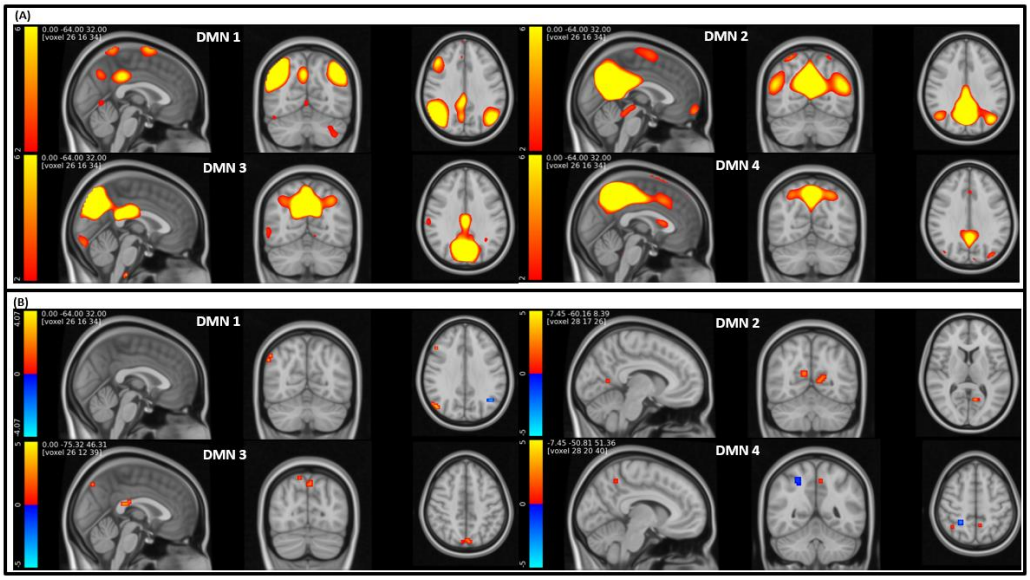

Figure 6: (A)Visualization of DMN spatial maps extracted from ICA order 80. (B) brain regions with significant group difference between HC and SZ in DMN area extracted from ICA order 80 after adoptive thresholding technique (p<0.01)

4. Discussion:

Studying brain functional connectivity has improved our understanding of brain functions and the impact of brain disorders. However, currently, studying functional connectivity disregards functional connectivity across multiple spatial scales. At best, apply multimodal ICA (Armin Iraji

et al., 2022)to study functional interactions but they do not construct the spatial hierarchy and do not impose direct constraints on the size of ICNs. In this work, we introduced telescopic ICA as an effective and adaptive tool to identify ICNs and construct spatial functional hierarchies and estimate functional sources across multiple spatial. We also leveraged the approach to study group comparison between HC and SZ which have been understudied as most research focuses on only single spatial scale.

Using telescopic ICA, we identified five distinct DMNs, including the original network extracted from DMN scale1 and its decomposition in four small networks from DMN scale2. (3.1) supports the finding that how the telescopic ICA approach captures bigger network in the first scale and uses its information to extract smaller networks in the next scale.

We observed in (3.2) that DMN in the first scale demonstrates a commendable mean reliability of 0.97, highlighting its robustness in effectively detecting the overall DMN. Additionally, the networks in the second scale exhibit reasonably high mean reliabilities, ranging from 0.80 to 0.91, indicating some variability in these more detailed functional sources. Our finding aligns with the observed pattern in a high model order ICA approach (Abou-Elseoud et al., 2010).

We observed a more pronounced group effect was observed in Scale 2 in comparison to Scale (3.3). Additionally, the results indicate that subject-level estimates exhibit greater similarity to both the reference and each other in Scale 2 as opposed to Scale 1(Figure 4), implying a more accurate estimation of networks. These collective findings suggest that the second scale may be more sensitive in capturing the group effect associated with SZ. Therefore, the telescopic ICA approach holds promise in identifying biomarkers for schizophrenia.

Previous studies show higher model order ICA results in more spatially granular ICNs (E. A. Allen et al., 2011; A. Iraji et al., 2022); however, (3.4) show that the DMNs captured by telescopic ICA approach are different from a single scale ICA with high model order. Also, more significant group differences captured using telescopic ICA approach compared to high model order ICA. These results also emphasis the importance of studying functional brain network in multi-scale using telescopic ICA approach.

In this study, we focus on only two scales with ICA model order 20 and 4 to capture network. Further studies can develop our approach in incremental scales to effectively capture ICNs in multiscale. Furthermore, future studies can explore differences across the different back-

reconstruction approaches (Erhardt et al., 2011). Here, we also focused on the voxel-wise group comparison of DMN spatial maps. Future studies should focus on telescopic ICA approach using static functional network connectivity, and dynamic functional network connectivity on DMN as well as other brain networks(Armin Iraji et al., 2022) .

5. Conclusion:

Brain functional connectivity can occur at different spatial scales, which has been underappreciated. Here we proposed a telescopic ICA approach as a new tool to construct spatial functional hierarchies of brain and estimate functional sources across multiple spatial scales. Our results on DMN show that our approach can capture replicable comprehensive spatial maps. Moreover, the telescopic ICA can detect significant group differences between HC and SZ that are missed using studying brain networks in single scale highlighting that our proposed approach represents a promising new tool for studying functional sources.

6. Author contribution:

Shiva Mirzaeian: Conceptualization; Methodology; Visualization; Writing-Original Draft. Ashkan Faghiri: Writing- Review & Editing. Vince Calhoun: Conceptualization; Investigation; Supervision; Writing- Review & Editing. Armin Iraji: Conceptualization; Investigation; Supervision; Writing- Review & Editing.

7. Acknowledgements:

Data collection was supported by the National Center for resources at the National Institute of Health [grant numbers: NIH 1 U24 RR021992, NIH 1 U24 RR025736-01].

8. Funding Information:

Vince D. Calhoun, National Institutes of Health, grant numbers: NIH R01MH123610. Vince D. Calhoun, National Science Foundation, grant numbers: NSF 2112455

9. References:

Abou-Elseoud, A., Starck, T., Remes, J., Nikkinen, J., Tervonen, O., & Kiviniemi, V. (2010). The effect of model order selection in group PICA. *Hum Brain Mapp*, *31*(8), 1207-1216. https://doi.org/10.1002/hbm.20929

Adali, T., Kantar, F., Akhonda, M., Strother, S., Calhoun, V. D., & Acar, E. (2022). Reproducibility in Matrix and Tensor Decompositions: Focus on Model Match, Interpretability, and Uniqueness. *IEEE Signal Process Mag*, *39*(4), 8-24. https://doi.org/10.1109/msp.2022.3163870

Allen, E., Erhardt, E., Damaraju, E., Gruner, W., Segall, J., Silva, R., Havlicek, M., Rachakonda, S., Fries, J., Kalyanam, R., Michael, A., Caprihan, A., Turner, J., Eichele, T., Adelsheim, S., Bryan, A., Bustillo, J., Clark, V., Feldstein Ewing, S., . . . Calhoun, V. (2011). A Baseline for the Multivariate Comparison of Resting-State Networks [Original Research]. *Frontiers in Systems Neuroscience*, *5*. https://doi.org/10.3389/fnsys.2011.00002

Allen, E. A., Damaraju, E., Plis, S. M., Erhardt, E. B., Eichele, T., & Calhoun, V. D. (2014). Tracking whole-brain connectivity dynamics in the resting state. *Cereb Cortex*, *24*(3), 663-676. https://doi.org/10.1093/cercor/bhs352

Allen, E. A., Erhardt, E. B., Damaraju, E., Gruner, W., Segall, J. M., Silva, R. F., Havlicek, M., Rachakonda, S., Fries, J., Kalyanam, R., Michael, A. M., Caprihan, A., Turner, J. A., Eichele, T., Adelsheim, S., Bryan, A. D., Bustillo, J., Clark, V. P., Feldstein Ewing, S. W., . . . Calhoun, V. D. (2011). A baseline for the multivariate comparison of resting-state networks. *Front Syst Neurosci*, *5*, 2. https://doi.org/10.3389/fnsys.2011.00002

Association, A. P. (2013). *Diagnostic and statistical manual of mental disorders*. American Psychiatric Association.

Beckmann, C. F., DeLuca, M., Devlin, J. T., & Smith, S. M. (2005). Investigations into resting-state connectivity using independent component analysis. *Philos Trans R Soc Lond B Biol Sci*, *360*(1457), 1001-1013. https://doi.org/10.1098/rstb.2005.1634

Bell, A. J., & Sejnowski, T. J. (1995). An information-maximization approach to blind separation and blind deconvolution. *Neural Comput*, *7*(6), 1129-1159. https://doi.org/10.1162/neco.1995.7.6.1129

Calhoun, V. D., & Adalı, T. (2012). Multisubject independent component analysis of fMRI: a decade of intrinsic networks, default mode, and neurodiagnostic discovery. *IEEE Rev Biomed Eng*, *5*, 60-73. https://doi.org/10.1109/rbme.2012.2211076

Calhoun, V. D., Adali, T., Pearlson, G. D., & Pekar, J. J. (2001). A method for making group inferences from functional MRI data using independent component analysis. *Hum Brain Mapp*, *14*(3), 140-151. https://doi.org/10.1002/hbm.1048

Calhoun, V. D., & de Lacy, N. (2017). Ten Key Observations on the Analysis of Resting-state Functional MR Imaging Data Using Independent Component Analysis. *Neuroimaging Clin N Am*, *27*(4), 561-579. https://doi.org/10.1016/j.nic.2017.06.012

Calhoun, V. D., Kiehl, K. A., & Pearlson, G. D. (2008). Modulation of temporally coherent brain networks estimated using ICA at rest and during cognitive tasks. *Hum Brain Mapp*, *29*(7), 828-838. https://doi.org/10.1002/hbm.20581

Calhoun, V. D., Liu, J., & Adali, T. (2009). A review of group ICA for fMRI data and ICA for joint inference of imaging, genetic, and ERP data. *Neuroimage*, *45*(1 Suppl), S163-172. https://doi.org/10.1016/j.neuroimage.2008.10.057

Clementz, B. A., Sweeney, J. A., Hamm, J. P., Ivleva, E. I., Ethridge, L. E., Pearlson, G. D., Keshavan, M. S., & Tamminga, C. A. (2016). Identification of Distinct Psychosis Biotypes Using Brain-Based Biomarkers. *Am J Psychiatry*, *173*(4), 373-384. https://doi.org/10.1176/appi.ajp.2015.14091200

Dalsgaard, S., Thorsteinsson, E., Trabjerg, B. B., Schullehner, J., Plana-Ripoll, O., Brikell, I., Wimberley, T., Thygesen, M., Madsen, K. B., Timmerman, A., Schendel, D., McGrath, J. J., Mortensen, P. B., & Pedersen, C. B. (2020). Incidence Rates and Cumulative Incidences of the Full Spectrum of Diagnosed Mental Disorders in Childhood and Adolescence. *JAMA Psychiatry*, *77*(2), 155-164. https://doi.org/10.1001/jamapsychiatry.2019.3523

Doucet, G., Naveau, M., Petit, L., Delcroix, N., Zago, L., Crivello, F., Jobard, G., Tzourio-Mazoyer, N., Mazoyer, B., Mellet, E., & Joliot, M. (2011). Brain activity at rest: a multiscale hierarchical

functional organization. *J Neurophysiol*, *105*(6), 2753-2763. https://doi.org/10.1152/jn.00895.2010

Erhardt, E. B., Rachakonda, S., Bedrick, E. J., Allen, E. A., Adali, T., & Calhoun, V. D. (2011). Comparison of multi-subject ICA methods for analysis of fMRI data. *Hum Brain Mapp*, *32*(12), 2075-2095. https://doi.org/10.1002/hbm.21170

Friston, K. J., & Frith, C. D. (1995). Schizophrenia: a disconnection syndrome? *Clin Neurosci*, *3*(2), 89-97.

Genon, S., Reid, A., Langner, R., Amunts, K., & Eickhoff, S. B. (2018). How to Characterize the Function of a Brain Region. *Trends Cogn Sci*, *22*(4), 350-364. https://doi.org/10.1016/j.tics.2018.01.010

Gorgolewski, K., Storkey, A., Bastin, M., & Pernet, C. (2012). Adaptive thresholding for reliable topological inference in single subject fMRI analysis [Methods]. *Frontiers in Human Neuroscience*, *6*. https://doi.org/10.3389/fnhum.2012.00245

Herzog, R., Rosas, F. E., Whelan, R., Fittipaldi, S., Santamaria-Garcia, H., Cruzat, J., Birba, A., Moguilner, S., Tagliazucchi, E., Prado, P., & Ibanez, A. (2022). Genuine high-order interactions in brain networks and neurodegeneration. *Neurobiology of Disease*, *175*, 105918. https://doi.org/https://doi.org/10.1016/j.nbd.2022.105918

Himberg, J., Hyvärinen, A., & Esposito, F. (2004). Validating the independent components of neuroimaging time series via clustering and visualization. *Neuroimage*, *22*(3), 1214-1222. https://doi.org/10.1016/j.neuroimage.2004.03.027

Iraji, A., Calhoun, V. D., Wiseman, N. M., Davoodi-Bojd, E., Avanaki, M. R. N., Haacke, E. M., & Kou, Z. (2016). The connectivity domain: Analyzing resting state fMRI data using feature-based data-driven and model-based methods. *Neuroimage*, *134*, 494-507. https://doi.org/10.1016/j.neuroimage.2016.04.006

Iraji, A., Deramus, T. P., Lewis, N., Yaesoubi, M., Stephen, J. M., Erhardt, E., Belger, A., Ford, J. M., McEwen, S., Mathalon, D. H., Mueller, B. A., Pearlson, G. D., Potkin, S. G., Preda, A., Turner, J. A., Vaidya, J. G., van Erp, T. G. M., & Calhoun, V. D. (2019). The spatial chronnectome reveals a dynamic interplay between functional segregation and integration. *Hum Brain Mapp*, *40*(10), 3058-3077. https://doi.org/10.1002/hbm.24580

Iraji, A., Faghiri, A., Fu, Z., Rachakonda, S., Kochunov, P., Belger, A., Ford, J. M., McEwen, S., Mathalon, D. H., Mueller, B. A., Pearlson, G. D., Potkin, S. G., Preda, A., Turner, J. A., van Erp, T. G. M., & Calhoun, V. D. (2022). Multi-spatial-scale dynamic interactions between functional sources reveal sex-specific changes in schizophrenia. *Network Neuroscience*, *6*(2), 357-381. https://doi.org/10.1162/netn_a_00196

Iraji, A., Faghiri, A., Fu, Z., Rachakonda, S., Kochunov, P., Belger, A., Ford, J. M., McEwen, S., Mathalon, D. H., Mueller, B. A., Pearlson, G. D., Potkin, S. G., Preda, A., Turner, J. A., van Erp, T. G. M., & Calhoun, V. D. (2022). Multi-spatial-scale dynamic interactions between functional sources reveal sex-specific changes in schizophrenia. *Netw Neurosci*, *6*(2), 357-381. https://doi.org/10.1162/netn_a_00196

Iraji, A., Faghiri, A., Lewis, N., Fu, Z., Rachakonda, S., & Calhoun, V. D. (2021). Tools of the trade: estimating time-varying connectivity patterns from fMRI data. *Soc Cogn Affect Neurosci*, *16*(8), 849-874. https://doi.org/10.1093/scan/nsaa114

Iraji, A., Fu, Z., Faghiri, A., Duda, M., Chen, J., Rachakonda, S., DeRamus, T., Kochunov, P., Adhikari, B. M., Belger, A., Ford, J. M., Mathalon, D. H., Pearlson, G. D., Potkin, S. G., Preda, A., Turner, J. A., van Erp, T. G. M., Bustillo, J. R., Yang, K., . . . Calhoun, V. D. (2023). Identifying canonical and replicable multi-scale intrinsic connectivity networks in 100k+ resting-state fMRI datasets. *Hum Brain Mapp*, *44*(17), 5729-5748. https://doi.org/10.1002/hbm.26472

Kahn, R. S., Sommer, I. E., Murray, R. M., Meyer-Lindenberg, A., Weinberger, D. R., Cannon, T. D., O'Donovan, M., Correll, C. U., Kane, J. M., van Os, J., & Insel, T. R. (2015). Schizophrenia. *Nat Rev Dis Primers*, *1*, 15067. https://doi.org/10.1038/nrdp.2015.67

Lee, T. W., Girolami, M., & Sejnowski, T. J. (1999). Independent component analysis using an extended infomax algorithm for mixed subgaussian and supergaussian sources. *Neural Comput*, *11*(2), 417-441. https://doi.org/10.1162/089976699300016719

Li, H., Zhu, X., & Fan, Y. (2018). Identification of Multi-scale Hierarchical Brain Functional Networks Using Deep Matrix Factorization. *Med Image Comput Comput Assist Interv*, *11072*, 223-231. https://doi.org/10.1007/978-3-030-00931-1_26

Li, Q., Calhoun, V., Ballem, A., Iraji, A., Yu, S., & Malo, J. (2023). Aberrant High-Order Dependencies in Schizophrenia Resting-State Functional MRI Networks. https://doi.org/10.48550/arXiv.2310.17445

Meng, X., Iraji, A., Fu, Z., Kochunov, P., Belger, A., Ford, J., McEwen, S., Mathalon, D. H., Mueller, B. A., Pearlson, G., Potkin, S. G., Preda, A., Turner, J., Erp, T. V., Sui, J., & Calhoun, V. D. (2022). Multimodel Order Independent Component Analysis: A Data-Driven Method for Evaluating Brain Functional Network Connectivity Within and Between Multiple Spatial Scales. *Brain Connect*, *12*(7), 617-628. https://doi.org/10.1089/brain.2021.0079

Meng, X., Iraji, A., Fu, Z., Kochunov, P., Belger, A., Ford, J. M., McEwen, S., Mathalon, D. H., Mueller, B. A., Pearlson, G., Potkin, S. G., Preda, A., Turner, J., van Erp, T. G. M., Sui, J., & Calhoun, V. D. (2023). Multi-model order spatially constrained ICA reveals highly replicable group differences and consistent predictive results from resting data: A large N fMRI schizophrenia study. *Neuroimage Clin*, *38*, 103434. https://doi.org/10.1016/j.nicl.2023.103434

National Academies of Sciences, E., Medicine, Policy, Global, A., Committee on Science, E. M., Public, P., Board on Research, D., Information, Division on, E., Physical, S., Committee on, A., Theoretical, S., Board on Mathematical, S., Analytics, Division on, E., Life, S., Nuclear, Radiation Studies, B., Division of, B., . . . Replicability in, S. (2019). In *Reproducibility and Replicability in Science*. National Academies Press (US)

Copyright 2019 by the National Academy of Sciences. All rights reserved. https://doi.org/10.17226/25303

Ochoa, S., Usall, J., Cobo, J., Labad, X., & Kulkarni, J. (2012). Gender differences in schizophrenia and first-episode psychosis: a comprehensive literature review. *Schizophr Res Treatment*, *2012*, 916198. https://doi.org/10.1155/2012/916198

Paus, T., Keshavan, M., & Giedd, J. N. (2008). Why do many psychiatric disorders emerge during adolescence? *Nat Rev Neurosci*, *9*(12), 947-957. https://doi.org/10.1038/nrn2513

Potkin, S. G., & Ford, J. M. (2009). Widespread cortical dysfunction in schizophrenia: the FBIRN imaging consortium. *Schizophr Bull*, *35*(1), 15-18. https://doi.org/10.1093/schbul/sbn159

Van Den Heuvel, M. P., & Fornito, A. (2014). Brain networks in schizophrenia. *Neuropsychology review*, *24*, 32-48.

van den Heuvel, M. P., & Hulshoff Pol, H. E. (2010). Exploring the brain network: a review on resting-state fMRI functional connectivity. *Eur Neuropsychopharmacol*, *20*(8), 519-534. https://doi.org/10.1016/j.euroneuro.2010.03.008